

Surface states, surface magnetization, and electron spin polarization: Fe(001)

C. S. Wang

Department of Physics and Astronomy, University of Maryland, College Park, Maryland 20742
and Physics Department and Materials Research Center, Northwestern University,
Evanston, Illinois 60201

A. J. Freeman

Physics Department, Northwestern University, Evanston, Illinois 60201
and Argonne National Laboratory, Argonne, Illinois 60439

(Received 8 June 1981)

Results are presented of an *ab initio* self-consistent spin-polarized energy-band study of a seven-layer ferromagnetic Fe(001) film to determine the energy dispersion and spatial character of surface states and their effects on the surface spin polarization, surface magnetic moment, and average exchange splitting. Band structures and surface states, layer density of states, and charge and spin densities are presented and used to discuss the surface effects in the interpretation of a number of experiments. A substantial enhancement of the surface-layer magnetic spin moment from its bulk value is found on Fe(001) which is in sharp contrast to the 20% reduction reported in our earlier study of a nine-layer Ni(001) film. Both of these results are consistent with available experimental information.

I. INTRODUCTION

The study of the magnetism of surfaces has attracted considerable experimental and theoretical interest because of the interesting phenomena associated with the existence of surface states (SS). In addition, the possible important role of surface phenomena in reconciling differences between electron-spin polarization experiments and self-consistent (SC) band structures for bulk systems has been recognized in recent years and this has led to more intensified theoretical efforts to describe the electronic structure of surfaces. These investigations use the bulk-energy-band method in the local spin-density-functional formalism as extended to the case of a thin film to simulate surface effects on a semi-infinite solid. A number of thin-film studies¹⁻¹⁰ have shown that (1) due to the localized nature of the $3d$ electrons, the charge density on transition-metal surfaces converges rather rapidly as the film thickness increases and (2) since the surface effects depend crucially on the existence, role, and nature of the SS, which are highly sensitive to details of the surface potential, only SC energy-band calculations can be relied upon to properly provide this information.

Recently we presented a SC numerical basis-set linear combination of atomic orbitals (LCAO)

discrete variational method which has proved to be a powerful tool with which to study surface properties (including chemisorption bonding and surface magnetism) through its successful application to one-, three-, and five-layer paramagnetic Ni(001) films,¹ oxygen chemisorbed in the $c(2 \times 2)$ configuration on Ni(001),² and a nine-layer ferromagnetic Ni(001) film.³ For the case of ferromagnetic Ni, we determined the spin-polarized SC band structure of a nine-layer Ni(001) film that is thick enough to accurately determine the energy dispersion and spatial character of SS and their effects on the surface spin polarization, charge distribution, and layer-projected density of states (DOS). Among our major results, we found a pair of majority spin \bar{M}_3 SS which split away from the bulk bands and cross the Fermi energy, E_F . This creates a majority spin d hole which decreases the surface-layer spin magnetization ($0.44\mu_B$) and the exchange splitting (0.41 eV at \bar{M}_3 SS) from their values ($0.58\mu_B$ and 0.63 eV) for bulk ferromagnetic Ni.¹¹ This slight reduction in the surface-layer magnetic moment is consistent with field emission¹² experiments. No evidence was found for magnetically "dead" layers on Ni(001) surfaces.¹³

This paper presents the results of an extension of our spin-polarized *ab initio* SC energy-band studies to the case of a ferromagnetic Fe(001) surface.

Among our results, we find that the spin density shows a strong Friedel-type oscillation which results in a substantially enhanced magnetization at the surface-layer plane. A much stronger surface-spin magnetic moment on Fe(001) is in sharp contrast to the 20% reduction that we found on the Ni(001) surface. In addition, we find a high density of SS to lie between the bonding and antibonding d -band complex and, in the case of minority spin, to coincide with the E_F . Some of these results may be generalized to interpret experiments performed on other surfaces of Fe where SC spin-polarized band structures are not currently available. By comparison with bulk results, the surface effects on the interpretation of a number of experiments (including angle-resolved photoemission,¹⁴ spin-polarized photoemission,¹⁵ spin-polarized tunneling,¹⁶ Mössbauer spectroscopy,¹⁷ electron capture,¹⁸ and anomalous Hall effects¹⁹) are discussed. In all cases studied we find our results to be in good qualitative agreement with experiment.

II. METHOD

We use our new SC linear combination of atomic orbitals method for an unsupported thin film,¹ and a numerical basis set ($3d$, $4s$, and $4p$) orthogonalized to the (frozen) core wave functions and symmetrized according to the symmetry of the two-dimensional (2D) wave vector \bar{k} . The non-muffin-tin crystal Coulomb potential is constructed as a superposition of overlapping spherically symmetric atomic potentials; correspondingly, a superposition of atomic charge densities is used to compute the local spin-density-functional exchange and correlation potential of von Barth and Hedin.²⁰ Atoms up to 25 a.u. from the origin are included in the direct lattice vector sums to construct the superposition potential and Bloch functions. Hamiltonian and overlap matrix integrals are evaluated accurately by means of a numerical three-dimensional Diophantine integration. From solutions of the secular equation, the charge and spin densities are calculated by a linear analytical triangle scheme (described earlier)¹ based on a sampling of 15 \bar{k} points in 1/8th of the 2D Brillouin zone (BZ). In this scheme, the irreducible wedge of the BZ is divided into 16 triangles, the energies of each spin (ordered separately for states of even and odd symmetry with respect to reflection symmetry about the center plane) are extrapolated linearly inside each triangle and the cutoff of the E_F is incorporated exactly within the linear-energy approxi-

mation.

Self-consistency is obtained iteratively within the superposition of a spherically symmetric atomic charge and spin-density model with the atomic configuration as an adjustable fitting parameter. The final SC potential minimizes the integrated rms difference between the input superposition and output crystal charge densities (0.478 compared to 56 valence electrons in the unit cell). In the last iteration, the layer-integrated input and output charge and spin densities agree to within 0.03 electrons and $0.03\mu_B$, respectively. As we discussed in Ref. 3, these values may be considered as the maximum limiting uncertainties in the charge and spin densities due to the extreme sensitivity of the output charge density with respect to small changes in the input charge density in the iterative procedure toward self-consistency.

III. RESULTS

A. Energy-band structure and surface states

The majority- and minority-spin energy bands along the high-symmetry directions in the 2D BZ are shown in Fig. 1. In order to clarify the already complex band structure, states of $\bar{\Delta}_2$ - \bar{Y}_2 - $\bar{\Sigma}_2$ symmetry are displayed separately above those of $\bar{\Delta}_1$ - \bar{Y}_1 - $\bar{\Sigma}_1$ symmetry. In addition, the wave functions have either even or odd parity with respect to reflection about the central plane. For a given 2D symmetry, only bands of opposite parity are allowed to cross one another.

In this figure, the pairs of even and odd symmetry SS are denoted either as circles or as triangles pointing toward each other if their degeneracy is split due to the finite thickness of the film. Based on Mulliken charge analysis, they indicate states with more than 70% of their charge localized on the first two surface layers.

The very important role of SS in modifying the surface magnetization from its bulk value has been demonstrated earlier in our study of a nine-layer spin-polarized Ni(001) film.³ Simply put, the Fermi surfaces are modified as the SS split away from the bulk continuum of states near E_F . In some cases additional electron or hole pockets are created. Since SS are localized near the surface by definition, only the top few atomic-layer spin magnetic moments are affected. A very important result shown in Fig. 1(a) is the position of E_F at the top of the majority-spin d -band complex with practically no band gap and hence no SS in the vicinity.

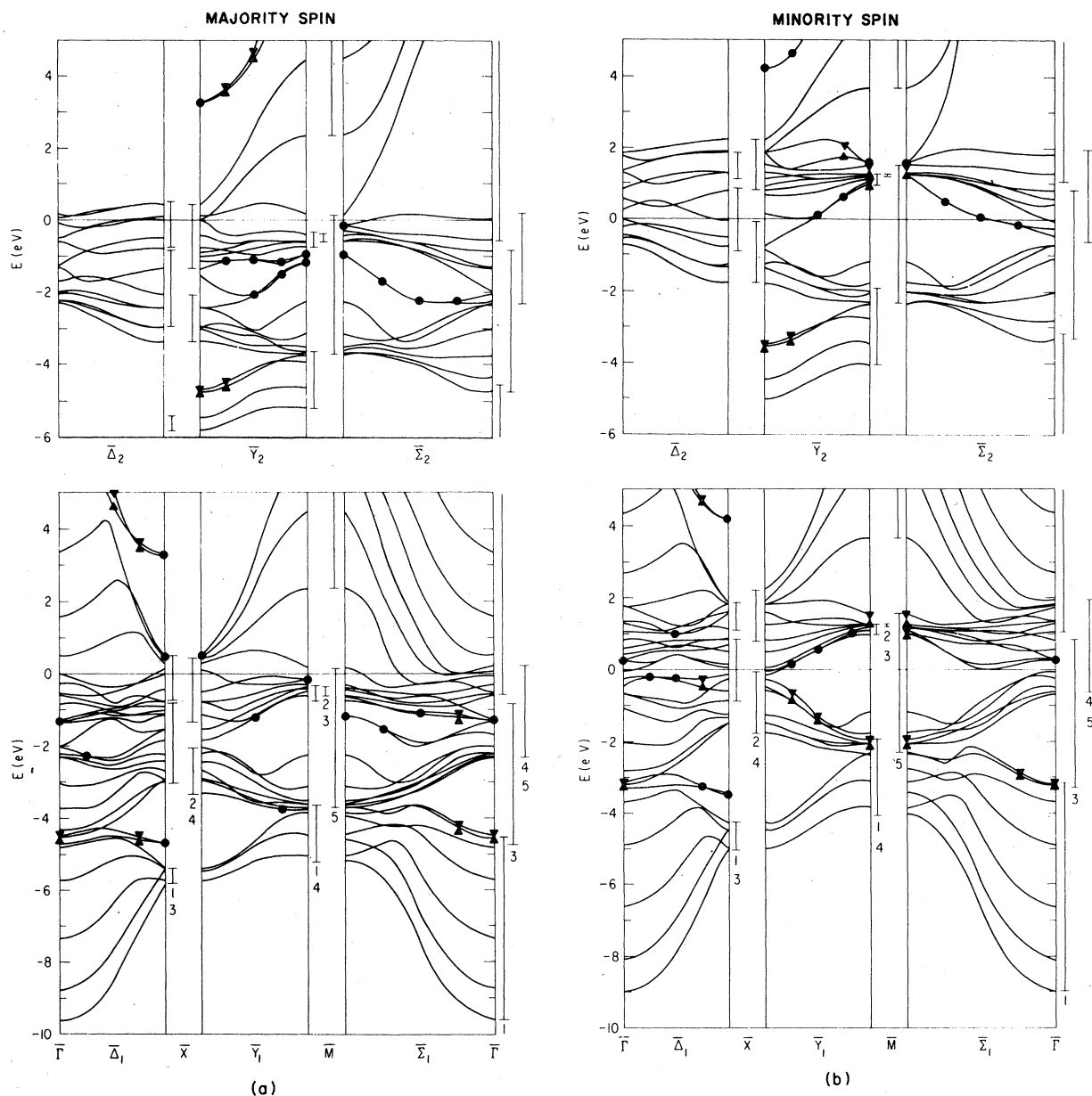


FIG. 1. (a) Majority-spin and (b) minority-spin energy bands of seven-layer Fe(001) film along the high-symmetry directions in the two-dimensional BZ. States of $\bar{\Delta}_2$ - \bar{Y}_2 - $\bar{\Sigma}_2$ and $\bar{\Delta}_1$ - \bar{Y}_1 - $\bar{\Sigma}_1$ symmetry are shown in the top and bottom panels, respectively. SS with more than 70% of their charge localized on the first two surface layers are indicated by circles and triangles.

By contrast, in Fig. 2(b), E_F lies in the middle of a large minority-spin band gap centered at $M_{1,4}$ and intercepts several SS of \bar{Y}_2 , $\bar{\Sigma}_2$, and \bar{Y}_1 symmetries. These SS give rise to a sharp peak in the minority-spin surface-projected DOS at E_F and are mostly responsible for the enhancement of the surface-layer magnetization on the Fe(001) surface.

B. Density of states

The layer by layer DOS projected by a Mulliken analysis and smoothed by a Gaussian broadening function of 0.3 eV full width at half maximum are shown in Fig. 2. The center plane DOS agrees very well with the bulk results of Callaway and

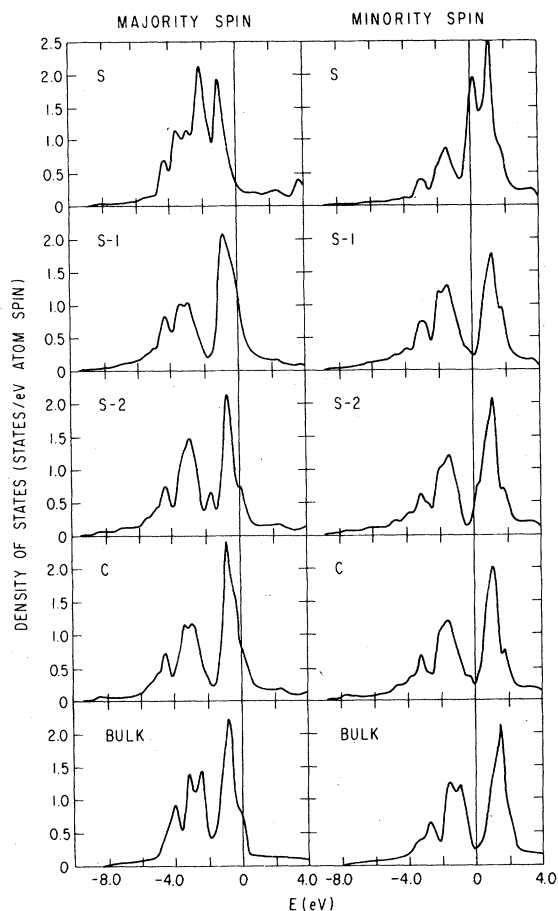


FIG. 2. Layer-projected DOS including a Gaussian broadening function of 0.3 eV full width at half maximum (FWHM). The bulk DOS of Wang and Callaway (Ref. 21) for ferromagnetic Fe is shown in the bottom panel for comparison.

Wang²¹ (bottom panels) while the surface plane DOS shows some narrowing of the d -band width and shifts of peak positions. As indicated in the top panels, and made more explicit in Fig. 3 which plots the difference between the surface and center layer DOS, there is a high density of SS between the bonding and antibonding d -band complex. As can be seen in Figs. 2 and 3, E_F lies in the valley of minority-spin bulk DOS (bottom panel on the right of Fig. 2) which coincides with the maximum of the corresponding surface-projected DOS (top panel on the right). This result, which can be generalized to other surfaces of Fe, has profound influences in the interpretation of many experiments (not necessarily limited to the (001) surface), as discussed in the following sections. Other interesting consequences include possible surface phase transitions,¹⁰ changes in superconducting transition tem-

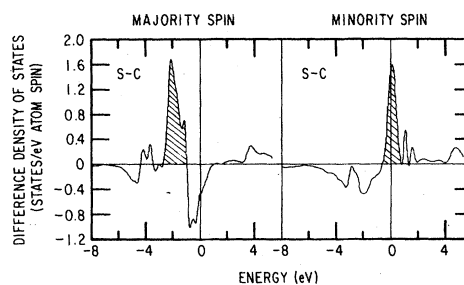


FIG. 3. Difference between the surface and center layer DOS of seven-layer Fe(001) film. A Gaussian broadening function of 0.3 eV FWHM has been included.

peratures, magnetism,²² etc., due to the enhancement of the DOS at E_F near the surface. These enhancements are most likely to occur near the middle of the transition-metal series where E_F lies in the valley of the d -electron bulk DOS; hence the resulting maximum of the corresponding surface DOS.

It is interesting to note that in Fig. 2, and more explicitly by cross-hatched lines in Fig. 3, some of the SS, which lie in the valley of the bulk DOS, penetrate two layers below the surface (the atom right below the surface atom in the bcc structure) as can be seen in the S-2 panel. This deeper penetration of the SS, not noticeable in our earlier studies of the Ni(001) surface,³ probably reflects a stronger surface perturbation of the more open bcc structure where 50% of the nearest neighbors of a surface atom are missing compared to a moderate 33% on the fcc Ni(001) surface. In order to conserve surface charge neutrality, these SS are usually accompanied by a reduction of the lower bonding and sometimes higher antibonding d -electron DOS as indicated by the negative differences between the surface and center layer DOS in Fig. 3. Thus the surface d -band width is narrower.

C. Charge densities, spin densities, and magnetic moments

As an indication of the results obtained, we show in Figs. 4 and 5 SC charge- and spin-density maps on the diagonal body of the cube (vertical axis along [001], i.e., on the (111) plane). As was found for the Ni(001) surface, the charge density starting at one layer below the surface plane is already bulklike. Our results, together with the SC charge densities found on other transition- and noble-metal surfaces,¹⁻¹⁰ confirm the important idea of "surface charge neutrality" which was widely

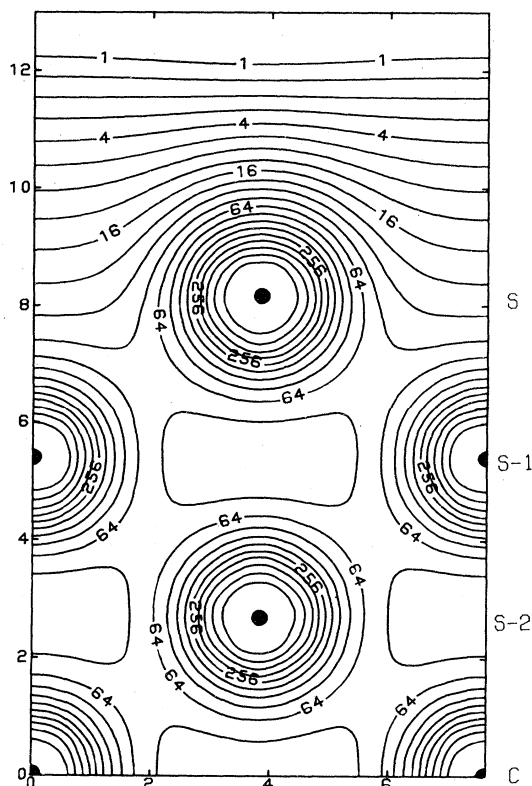


FIG. 4. The self-consistent charge-density map in units of 0.001 a.u. on the (110) plane. Each contour line differs by a factor of $\sqrt{2}$.

recognized in earlier non-self-consistent empirical LCAO calculations.²³ Similarly, suppression of the Friedel oscillation in the high-density limit was reported in an earlier jellium calculation.²⁴ This can be understood as follows: Owing to the localized nature of the 3*d* electrons, a very small amount of charge transfer in or out of the surface amounts to a fairly large surface dipole moment and an extremely long-range Coulomb potential. Thus, the final SC potential must maintain a very delicate balance of charge densities near the surface region. This is also the basic reason that self-consistency is so hard to achieve in transition metals. (In response to a very small change in the input potential, a very large amount of the charge is washed in and out of the surface and often leads to a divergence in the iterative procedure toward self-consistency.) This discussion also makes clear why the existence of some SS is so sensitive to small changes in the surface potential barrier.²⁵

In sharp contrast to the rapid healing rate of the charge densities, the spin densities shown in Fig. 5 exhibit a Friedel-type oscillation which penetrates

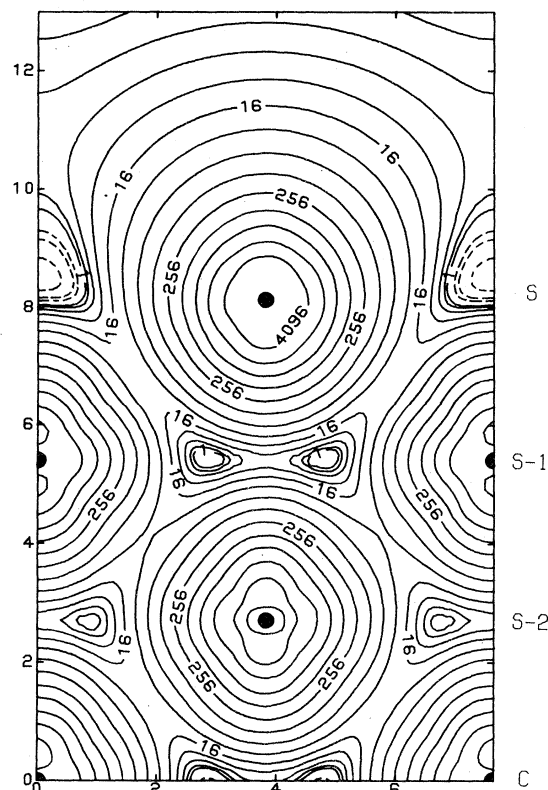


FIG. 5. Self-consistent spin-density map of seven-layer of Fe(001) in units of 0.0001 a.u. on the (110) plane. Each contour line differs by a factor of 2. The dashed lines indicate negative spin density.

several layers from the surface plane. This is possible because the spin density is determined entirely by the difference in exchange and correlation potential between the two spin states which is of much shorter range and is weaker in intensity than is the spin-independent Coulomb potential. [An example of the subtle differences between the Coulomb effect and the exchange-correlation potentials is seen in the differences in the SS on Ni(001) (Refs. 3 and 6) and Cu(001) (Ref. 5). As in Cu, the majority-spin Ni 3*d* states are filled, but the SS found on Ni(001) remain as weak as those of either the minority spin or the paramagnetic state while the SS on Cu(001) are extremely strong. Thus the different strength of the SS on Ni and Cu is determined primarily by their different charge densities and Coulomb potentials; the exchange splitting as a function of the spin density only plays a minor role.]

In good agreement with the bulk results,^{11,12} the spin density for a Ni(001) film³ is larger along the [101] direction than along [001] while the spin

density for an Fe(001) film is largest along the [001] direction with similar magnitudes along the [110] and [111] directions. Negative spin density, shown as dashed lines, was found throughout the interstitial region (including the surface layer) of Ni(001) but only along the [110] direction close to the surface and center planes on Fe(001) (cf. Fig. 5). Thus the spin density is positive in the outer part of the Fe(001) surface in contrast to that of Ni(001).

From the SC total charge and spin densities we may determine layer plane distributions by a nearest-volume numerical integration. Our results for the seven-layer Fe(001) film are tabulated in Table I together with our earlier calculation for a nine-layer Ni(001) film.³ Both calculations yield a practically neutral charge density around each atom while the spin density shows strong Friedel-type oscillations. In the case of Ni, the spin magnetic moments close to the center plane are in very good agreement with the experimental value²⁶ of $0.56\mu_B$ and are slightly smaller than the theoretical value ($0.58\mu_B$) for bulk Ni.¹¹ This was our original reason for choosing a seven-layer-thick film to study the Fe surface. Our results indicate, however, that a seven-layer Fe(001) film was not thick enough to stabilize the Friedel oscillation nor to yield the bulk magnetic-moment value for the center layer. Thus we may expect only a semi-quantitatively correct magnetic spin density at the surface layer. In our calculation, we find an *increase* from its bulk value²¹ of $2.16\mu_B$ to approximately $3\mu_B$. As can be seen from Table I, this result is in sharp contrast to the spin density on the Ni(001) surface layer which was found earlier to *decrease* to $0.42\mu_B$ from its bulk value of

$0.58\mu_B$. The relatively large surface magnetization of Fe(001) gave rise to some differences between the SS of the majority and minority spins which can be seen from the surface layer DOS shown in the top panel of Fig. 2. As we discussed earlier, such a difference was not seen in the surface layer DOS of Ni(001) because its surface spin magnetic moment is much smaller than that of Fe(001).

IV. COMPARISONS WITH EXPERIMENT

There are now a number of experimental results on ferromagnetic transition-metal surfaces which can be compared with the predictions of the calculations reported here. Of these, spin-polarized photoemission is one of the important experiments used to study the electron spin polarization (ESP) for ferromagnetic metals. Earlier measurements on polycrystalline samples of Ni, Fe, and Co showed positive ESP which were proportional to their magnetization.²⁷ The importance of using single-crystal surfaces was later demonstrated by Eib and Alvarado²⁸ who found a negative ESP for the Ni(001) surface that changed sign abruptly within 0.1 eV of the threshold. Near threshold, as Dempsey and Kleinman²⁹ pointed out, the conservation of the transverse component of the wave vector upon escape in the three-step photoemission process would limit the contribution to regions around $\bar{\Gamma}$ in the 2D BZ. Thus, although our surface DOS is dominated by minority-spin electrons at E_F , Fig. 1(b) shows that those SS lying halfway from the $\bar{\Gamma}$ point to the \bar{M} point along the $\bar{\Sigma}_2$ direction should not contribute greatly to ESP at threshold. We are not aware of any experimental data on the Fe(001) surface.

Recent measurements of Eib and Reihl¹⁵ on Fe(111) show a positive ESP (+60%) at E_F which drops linearly to 17% within 3 eV above threshold. This was interpreted as consistent with an itinerant model of ferromagnetism since the bulk DOS at E_F is predominantly of majority spin. As discussed earlier, we expect a large density of minority-spin SS at E_F to exist on all surfaces of Fe. These SS may not contribute much to ESP at threshold if the magnitude of their wave vectors are large; but they are important in accounting for the rapid drop of ESP away from the threshold where the ESP of the bulk DOS initially becomes more positive.

We have seen from Fig. 2 that the area below the majority-spin surface-projected DOS (top panels) integrated up to E_F is much larger than

TABLE I. Layer plane distribution of charge and spin densities for nine-layer of Ni(001) (Ref. 3) and seven-layer of Fe(001) films.

Layer	Ni(001)		Fe(001)	
	Charge	Spin	Charge	Spin
S	10.02	0.44	7.95	3.01
S-1	9.97	0.59	8.04	1.69
S-2	9.97	0.62	7.98	2.13
S-3	10.02	0.56		
C	10.05	0.54	8.06	1.84
Bulk	10.00	0.58 ^a	8.00	2.15 ^b

^aReference 11.

^bReference 21.

that below the center plane or bulk results (bottom panels), while the area below the minority-spin surface-projected DOS is smaller. Thus the surface magnetization on Fe(001) is substantially enhanced in contrast to the 20% reduction that we found on the Ni(001) surface (cf. Table I). This result seems to be supported by several experiments performed on different surfaces of Fe. Let us first consider the angle resolved photoemission experiment. In contrast to the results of Ni where the measured exchange splitting [0.3 eV (Ref. 30)] is only half of the theoretical prediction [0.6 eV (Ref. 11)] for the bulk system, the agreement between theory and experiment is, in general, rather good for Fe.¹⁴ The major deviation occurs along the Λ_3 - P_4 - F_3 direction where the exchange splitting at P_4 measured on the Fe(111) surface is larger than that of the theoretical value²¹ of 1.34 eV for the bulk system by approximately 0.3 eV. This result can be interpreted as an indication of the contribution from the relevant SS whose exchange splittings are increased due to the enhancement of the surface magnetization. Qualitatively, both of these results may be viewed as consistent with anomalous Hall-effect¹⁹ and spin-polarized tunneling¹⁶ experiments using ultrathin Ni, Fe, and Co films: These experiments agree in that Ni films become ferromagnetic only for films thicker than 2.5 atom layers while a monolayer of Fe or Co film already shows a magnetic moment. Further quantitative comparison of our results with ultrathin film measurements are limited by the possible influence of the interface between magnetic metal and nonmagnetic substrate. Nevertheless, our results clearly rule out the possibility of magnetic "dead layers" on Ni (Ref. 13) or Fe (Ref. 31) metal surfaces.

Of course, the interpretation of spin-polarized tunneling¹⁶ and field emission^{12,32} experiments depends importantly on the precise details of the *sp* electron-spin densities because the transition matrix element for the extended *sp* electrons may be considerably larger than those for the localized *d* electrons. We have seen above that the Fe(001) and Ni(001) spin densities show differing results, with the Ni(001) showing negative spin density throughout the interstitial region (including the surface layer) but only along the [110] direction on Fe(001).

Surface electron-spin densities may be probed by Mössbauer effect and electron-capture spectroscopy (ECS) studies. In ECS experiments,¹⁸ unpolarized swift deuterons impinge at grazing angles upon clean single crystalline ferromagnetic surfaces and capture spin-polarized electrons during reflection and thus probe the exponential tail of the electronic spin density at the surface. Recently, Rau¹⁸ reported that his measured spin polarization of -64% on Ni(001) surface agrees very well with our earlier values of -55% (versus the center plane value of -78%) for a nine-layer Ni(001) film. Our results for Fe(001) in Fig. 5 indicate only positive spin densities in the outer part of the surface regions, again in agreement with Rau's results which show only positive spin polarization in all directions.

Finally, enhanced surface magnetization on the Fe(001) surface was also inferred from recent Mössbauer measurements.¹⁷ A family of films with a total Fe thickness of 60 Å were constructed, made primarily of isotopically pure ⁵⁶Fe with a very thin layer (4–10 Å) of ⁵⁷Fe placed at different depths in the film. Bulk values of the hyperfine field of H_n were obtained for ⁵⁷Fe layers near the middle of the film and significantly enhanced values of H_n were obtained for ⁵⁷Fe layers near the surface of the film. Furthermore, they found that the average H_n for 20-Å-thick films at 4.2 K was greater than the bulk value. Both of these results are consistent with our prediction of an enhancement of surface spin magnetic moments on Fe(001).

ACKNOWLEDGMENTS

We are grateful to D. E. Ellis, D. D. Koelling, S. Bader, and M. Brodsky for helpful discussions and M. Brodsky for support and encouragement. This work was supported by the National Science Foundation (Grant No. DMR 77-23776) and under the NSF-MRL program through the Materials Research Center of Northwestern University, Grant No. DMR 79-23573 and the Department of Energy. One of us (C.S.W.) also would like to acknowledge the support of the Naval Research Laboratory through the Office of Naval Research Contract No. N00014-79-C-0558.

- ¹C. S. Wang and A. J. Freeman, Phys. Rev. 19, 793 (1979).
- ²C. S. Wang and A. J. Freeman, Phys. Rev. B 19, 4930 (1979).
- ³C. S. Wang and A. J. Freeman, Phys. Rev. B 21, 4585 (1980); J. Appl. Phys. 50, 1940 (1979); J. Magn. Mater. 15—18, 869 (1980).
- ⁴S. G. Louie, K. M. Ho, J. R. Chelikowsky, and M. L. Cohen, Phys. Rev. Lett. 37, 1289 (1976); Phys. Rev. B 15, 5627 (1977); G. P. Kerker, K. M. Ho, and M. L. Cohen, *ibid.* 18, 5473 (1978); Phys. Rev. Lett. 40, 1593 (1978); S. G. Louie, *ibid.* 40, 1525 (1978); 42, 476 (1979).
- ⁵J. G. Gay, J. R. Smith, and J. F. Arlinghaus, Phys. Rev. Lett. 42, 332 (1979); J. R. Smith, J. G. Gay, and F. J. Arlinghaus, Phys. Rev. B 21, 2201 (1980).
- ⁶F. J. Arlinghaus, J. G. Gay, and J. R. Smith, Phys. Rev. B 21, 2055 (1980).
- ⁷J. G. Gay, J. R. Smith, F. J. Arlinghaus, and T. W. Capehart, Phys. Rev. B 23, 1559 (1981).
- ⁸J. A. Appelbaum and D. R. Hamann, Solid State Commun. 27, 881 (1978); P. J. Feibelman and D. R. Hamann, *ibid.* 31, 413 (1979); P. J. Feibelman, J. A. Appelbaum, and D. R. Hamann, Phys. Rev. B 20, 1433 (1979).
- ⁹O. Jepsen, J. Madsen, and O. K. Anderson, J. Magn. Mater. 15—18, 867 (1980).
- ¹⁰H. Krakauer, M. Posternak, and A. J. Freeman, Phys. Rev. Lett. 43, 1885 (1979); M. Posternak, H. Krakauer, A. J. Freeman, and D. D. Koelling, Phys. Rev. B 21, 5601 (1980).
- ¹¹C. S. Wang and J. Callaway, Phys. Rev. B 15, 298 (1977).
- ¹²M. Landolt and M. Campagna, Phys. Rev. Lett. 38, 663 (1977).
- ¹³L. N. Liebermann, J. Clinton, D. M. Edwards, and J. Mathon, Phys. Rev. Lett. 25, 232 (1970).
- ¹⁴D. E. Eastman, F. J. Himpsel, and J. A. Knapp, Phys. Rev. Lett. 44, 95 (1980).
- ¹⁵W. Eib and B. Reihl, Phys. Rev. Lett. 40, 1674 (1978).
- ¹⁶R. Meservey, P. M. Tedrow, and V. R. Kalvey, Solid State Commun. 36, 969 (1980); J. Appl. Phys. 52, 1617 (1981).
- ¹⁷J. Tyson, A. H. Owens, J. C. Walker, and G. Bayreuther, J. Appl. Phys. 52, 2487 (1981).
- ¹⁸C. Rau, Comments Solid State Phys. 2, 177 (1980) and references therein.
- ¹⁹G. Bergmann, Phys. Rev. Lett. 41, 264 (1978).
- ²⁰U. von Barth and L. Hedin, J. Phys. C 5, 1679 (1972).
- ²¹J. Callaway and C. S. Wang, Phys. Rev. B 16, 2095 (1977).
- ²²D. R. Grempel and S. C. Ying, Phys. Rev. Lett. 45, 1018 (1980).
- ²³D. G. Dempsey, L. Kleinman, and Ed Caruthers, Phys. Rev. B 12, 2932 (1975); 13, 1489 (1976); 14, 279 (1976).
- ²⁴N. D. Lang and W. Kohn, Phys. Rev. B 1, 4555 (1970).
- ²⁵E. Caruthers and L. Kleinman, Phys. Rev. Lett. 35, 738 (1975).
- ²⁶H. Dannan, R. Herr, and A. J. P. Meyer, J. Appl. Phys. 39, 669 (1968).
- ²⁷G. Busch, M. Campagna, and H. C. Siegmann, Phys. Rev. B 4, 746 (1971).
- ²⁸W. Eib and S. F. Alvarado, Phys. Rev. Lett. 37, 444 (1978).
- ²⁹D. G. Dempsey and L. Kleinman, Phys. Rev. Lett. 39, 1297 (1977); D. G. Dempsey, W. R. Grise, and L. Kleinman, Phys. Rev. B 18, 1270 (1978).
- ³⁰D. E. Eastman, F. J. Himpsel, and J. A. Knapp, Phys. Rev. Lett. 40, 1514 (1978); F. J. Himpsel, J. A. Knapp, and D. E. Eastman, Phys. Rev. B 19, 2919 (1979).
- ³¹L. N. Liebermann, D. R. Fredkin, and H. B. Shore, Phys. Rev. Lett. 22, 539 (1969).
- ³²M. Landolt and Y. Yafet, Phys. Rev. Lett. 40, 1401 (1978).